Greenhouse Gas Emission Reduction in Residential Buildings: A Lightweight Model to be Deployed on Edge Devices

Paul Ortiz[a,*], Sylvain Kubler[a,b], Éric Rondeau[a], Katie McConky[c], Alexander Alexandrovich Shukhobodskiy[d], Giuseppe Colantuono[d], Jean-Philippe Georges[a]

[a] *Université de Lorraine, CNRS, CRAN, F-54000, France*
[b] *Interdisciplinary Centre for Security, Reliability and Trust, University of Luxembourg, L-1359 Esch-sur-Alzette, Luxembourg*
[c] *Department of Industrial and Systems Engineering, Rochester Institute of Technology, 81 Lomb Memorial Drive, Rochester, NY 14623, United States*
[d] *School of Built Environment, Engineering and Computing, Leeds Beckett University, Leeds, LS1 3HE, UK*

Abstract

Electricity produced and used in the residential sector is responsible for approximately 30% of the greenhouse gas emissions (GHGE). Insulating houses and integrating renewable energy and storage resources are key for reducing such emissions. However, it is not only a matter of installing renewable energy technologies but also of optimizing the charging/discharging of the storage units. A number of optimization models have been proposed lately to address this problem. However, they are often limited in several respects: (i) they often focus only on electricity bill reduction, placing GHGE reduction on the backburner; (ii) they rarely propose hybrid-energy storage optimization strategies considering thermal and storage heater units; (iii) they are often designed using Linear Programming (LP) or metaheuristic techniques that are computational intensive, hampering their deployment on edge devices; and (iv) they rarely evaluate how the model impacts on the battery lifespan. Given this state-of-affairs, the present article compares two approaches, the first one proposing an innovative sliding grid carbon intensity threshold algorithm developed as part of a European project named RED WoLF, the second one proposing an algorithm designed based on LP. The comparison analysis is carried out based on two distinct real-life scenarios in France and UK. Results show that both algorithms contribute to reduce GHGE compared to a solution without optimization logic (between 10 to 25%), with a slight advantage for the LP algorithm. However, RED WoLF makes it possible to reduce significantly the computational time ($\approx$ 25 min for LP against $\approx$ 1 ms for RED WoLF) and to extend the battery lifespan (4 years for LP against 12 years for RED WoLF).

Keywords: Greenhouse Gas Emission, Energy efficiency, Photovoltaics, Battery, Edge computing, Linear Programming

1. Introduction

Globally, the residential sector accounts for a substantial part of the consumed energy and greenhouse gas emission (GHGE) (Baek and Kim, 2020). Reducing GHGE can be achieved by better insulating houses and buildings, switching from polluting (albeit cheap) coal to natural gas or renewable energy sources (Lazarus and van Asselt, 2018), and developing intelligent applications to efficiently integrate such renewables resources with flexible storage systems (Ahmed et al., 2021). Indeed, it is not only a matter of installing renewable energy technologies (e.g., PV array, wind or biomass), but also of optimizing the charging/discharging of the storage units (e.g., battery, thermal storage, electric vehicles, etc.) (Al-Shahri et al., 2021).

A number of charging and discharging optimization models of storage units have been proposed in the literature (Hannan et al., 2021). Although these models may differ in terms of required infrastructure (e.g., different renewable energy sources, loads), targeted fitness goals, they are often limited in three-respects. First, they are often designed based on Linear Programming (LP), which can quickly become complex and time consuming with the increase in the number of constraints and variables. Significant computation requirements of LP can have negative environmental impacts due to computational energy consumption.

*Corresponding author
Email addresses: paul.ortiz@univ-lorraine.fr (Paul Ortiz), s.kubler@univ-lorraine.fr (Sylvain Kubler), eric.rondeau@univ-lorraine.fr (Éric Rondeau), ktmeie@rit.edu (Katie McConky), A.Shukhobodskiy@leedsbeckett.ac.uk (Alexander Alexandrovich Shukhobodskiy), G.Colantuono@leedsbeckett.ac.uk (Giuseppe Colantuono), jean-philippe.georges@univ-lorraine.fr (Jean-Philippe Georges)

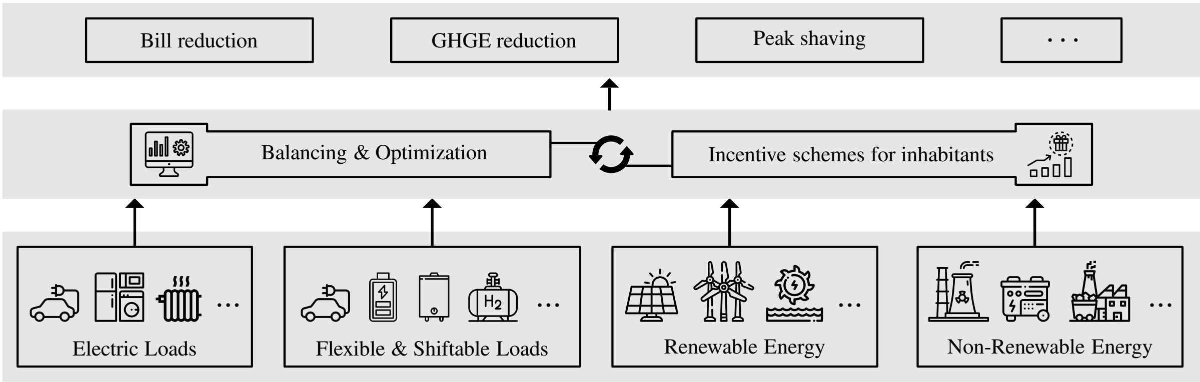

Figure 1: Nanogrid main technological constituents

Heuristic methods to solve LP's can combat the computation issue, but the trade off is in solution quality with heuristics providing sub-optimal solutions. Second, they often focus on cost – *electricity bill* – reduction, placing environmental goals such as GHGE reduction, maximization of the system's lifespan, on the backburner. Third, they often consider a single storage unit (mostly Battery Energy Storage System - BESS) and rarely propose hybrid-energy storage optimization strategies (e.g., combining BESS with thermal storage, storage heaters, *etc.*). Such limitations have been stressed and discussed in the recent survey published by Hannan et al. (2021). To overcome these limitations, an innovative sliding grid carbon intensity threshold approach, developed as part of a European project named RED WoLF[1] (Rethink Electricity Distribution Without Load Following), has been presented initially in (Shukhobodskiy and Colantuono, 2020), modified in (Ortiz et al., 2021) and extended with (Wiesheu et al., 2021), which can act on any dwelling. In the present article, the goal is to study the extent to which RED WoLF outperforms LP or heuristic-based algorithms in terms of GHGE reduction efficiency, battery lifespan maximization, and computational complexity. The latter (computational complexity) is of particular importance with the advent of Edge Computing in the energy sector (Munir et al., 2019), which pushes the frontier of computation applications away from centralized nodes (Cloud) to the communication network's extremes (Edge).

In section 2, a review of existing energy storage optimization strategies is carried out, based on which research trends and gaps are discussed. Section 3 presents the RED WoLF system and underlying logic, but also proposes an extension of the algorithm introduced by Olivieri and McConky (2020) with the aim of integrating PV energy resources into their model.

[1] https://www.nweurope.eu/projects/project-search/red-wolf-rethink-electricity-distribution-without-load-following/

Both algorithms are evaluated and compared in section 4 considering two real-life scenarios (houses) from France and UK, the conclusion follows in section 5. Overall, the present paper differs from our previous papers in several respects:

- first, an in-depth analysis and comparison between two approaches (rule-based *vs.* Linear programming) aiming at reducing carbon emission in residential houses are carried out. To the best of our knowledge, no study has ever conducted such an analysis in the field of low greenhouse gas emission houses.
- second, in order to allow for fair comparison between the two approaches, an extension of the initial Olivieri's model is proposed to integrate PV systems;
- third, even if the prime objective is to reduce CO_2, an in-depth analysis and comparison analysis of how the two models behave in terms of the battery lifespan and computational time needed to solve the problem are carried out.

2. Scope, Definition and Positioning

Section 2.1 gives the context of our contribution focusing on the energy field. Section 2.2 discusses how our research progresses the current state-of-the-art.

2.1. Scope and Definition

The energy life cycle consists of several stages, spanning from its generation and transmission to its distribution and consumption (Saleem et al., 2019). The present research falls within the scope of energy management at the consumption stage, and more exactly in residential nanogrids (Burmester et al., 2017). Energy management in nanogrids usually consists of four equipment categories, as depicted in Figure 1, namely:

- *Electric Loads:* referring to house equipment that consume energy such as appliances, Electric Vehicle (EV), HVAC equipment, *etc.*;

- *Flexible & Shiftable Loads:* referring to equipment able to store energy for later use (incl., batteries, storage heaters, water cylinders, or stationary electrical vehicles) or to shift consumption from the peak of the utility provider's demand curve, when energy is most precious, to another most appropriate time (e.g., by delaying the start time of the washing machine or the charging start time of the EV);

- *Renewable energy sources:* referring to energy sources that can be regenerated and sustainably utilized from nature including non-fossil energy such as wind energy, solar energy, biomass energy, geothermal energy or kinetic ocean energy;

- *Non-renewable energy sources:* referring to energy sources that have finite supplies and cannot be restored or regenerated in short periods of time (incl., coal, natural gas, oil, nuclear energy).

Depending on the type of nanogrid architecture (i.e., presence or not of renewable energy sources, flexible loads, *etc.*) and the targeted objectives (e.g., reducing energy bills and/or GHGE and/or extending device lifetimes, *etc.*), the Energy Management System (EMS) integrates different logics (Georgiou et al., 2019), as reviewed and discussed in the next section.

2.2. Current state-of-affairs

This section presents an overview of the current state-of-affairs, along with the trends and gaps in the literature. The methodology applied for reviewing the literature is detailed in Figure 2. Sources such as doctoral dissertations, master's theses, textbooks and unpublished papers were ignored. A first filter, denoted by (1) in Figure 2, has been applied, consisting in selecting articles based on the abstract content. This led us to keep 202 articles. A second filter, denoted by (2), has then been applied to keep papers dealing with energy storage optimization (147 articles were identified). A final third filter denoted by (3), was applied to keep only papers proposing approaches at the residential level only. This led us to review 43 articles, which have been classified in Table 1 based on the following criteria/categories:

- *Lifecycle phase:* highlights whether the proposed approach deals with an optimization problem at the Design (D) phase (e.g., for battery sizing) or at the Operational (O) one (i.e., for deciding when to consume/store/release energy);

- *Optimization goal(s):* highlights what objective(s) is/are targeted by the proposed approach, which are categorized as follows: (i) bill reduction; (ii) GHGE reduction; (iii) peak shaving; (iv) sustainability; (v) grid independency; (vi) fuel reduction;

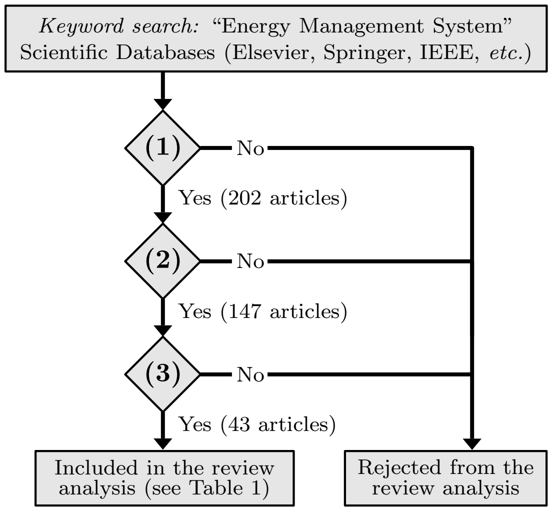

Figure 2: Literature review process

- *Energy storage:* highlights what storage systems are considered/used, which are categorized as follows: (i) BESS (battery energy storage system) to (ii) hydro, (iii) Electric Vehicle (EV), (iv) thermal or heating, and (v) fuel cell storage. This category also emphasizes whether the approach takes advantage of (vi) shiftable loads;

- *Energy production:* highlights what production systems are considered/used, which are categorized as follows: (i) fossil fuel, (ii) electrical grid; (iii) PV array; (iv) wind turbine;

- *Method:* highlights the type of methods used for optimization: (i) Heuristic (H); (ii) Metaheuristic (MH); (iii) Mathematical Programming (MP); (iv) Rule-Based (RB); (v) Multi-Criteria Decision Attribute (MCDA).

A first interesting finding from this review is that there is a similar proportion of articles dealing with optimization problems at the design (D) phase and at the operational (O) one. In the former (D), articles mainly focus on optimizing the hardware constituents (battery size, installation cost, self-consumption capabilities, *etc.*) as well as the equipment configuration to meet the various possible objectives (e.g., total cost of the installation, environmental impact, self-consumption). The HOMER (Hybrid Optimization Model for Electric Renewable) software, developed by the National Renewable Energy Laboratory (NREL), appears in several of these articles such as (Fodhil et al., 2019), as it allows for simulating and

Table 1: Classification of the scientific articles reviewed throughout Section

	Lifecycle Phase	Optimization Goals: Bill reduction	GHGE reduction	Peak Shaving	Sustainability	Grid Independency	Fuel reduction	Storage/Shiftable: Shiftable Load	BESS	Hydro	EV	Thermal / Heating	Fuel Cell	Production: Fosil Fuel	Electrical Grid	PV Array	Wind Turbine	Method
Tooryan et al. (2020a)	D	■	■		■	■	■		■			■	■	■	■	■	■	MH
Tooryan et al. (2020b)	D	■	■		■	■	■		■					■		■	■	MH
Das et al. (2020)	D	■	■		■	■		■			■				■			MCDA
Yazan M. et al. (2019)	D	■	■		■													MH
Awan et al. (2019)	D	■	■		■				■				■	■		■	■	MH
Ashraf et al. (2020)	D	■	■			■												MH
Awan (2019)	D	■	■			■			■					■		■	■	H
Fodhil et al. (2019)	D	■	■			■			■					■		■		MH
Fonseca et al. (2021)	D	■	■			■			■				■	■	■	■		MP
Ayse Fidan and Muhsin (2020)	D	■	■				■											MH
Bingham et al. (2019)	D	■	■						■						■	■		MH
Salehi et al. (2019)	D	■	■						■			■		■	■		■	RB
García-Vera et al. (2020)	D	■			■				■					■		■	■	MH
Aziz et al. (2019)	D	■							■	■				■		■		RB, H
Pandžić (2018)	D	■							■						■			MP
O'Shaughnessy et al. (2018)	D	■							■						■	■		H
Nguyen et al. (2014)	D	■													■		■	MP
Borra and Debnath (2019)	D		■				■							■				MH
Arévalo et al. (2020)	D																	RB
Bhayo et al. (2020)	D								■	■						■		MH
Haidar et al. (2018)	O	■	■						■					■	■			MP
Mahmud et al. (2018)	O	■	■						■		■				■	■		RB
Liu et al. (2020)	O	■	■		■				■						■	■		RB
Nagapurkar and Smith (2019)	O	■	■		■				■				■	■		■	■	MH
Olivieri and McConky (2020)	O	■	■						■						■			MP
Schram et al. (2020)	O	■	■		■	■			■						■			H
Stepaniuk et al. (2018)	O	■	■			■			■						■	■	■	RB
Terlouw et al. (2019a)	O	■	■		■				■						■	■		MP
Terlouw et al. (2019b)	O	■	■			■		■	■			■			■	■		MP
Moradi et al. (2016)	O	■	■						■					■	■	■	■	MP
Nottrott et al. (2013)	O	■		■		■			■						■	■		MP
Yadav et al. (2018)	O	■		■					■					■				MP
Mulleriyawage and Shen (2020)	O	■			■	■			■						■	■		MP
Litjens et al. (2018)	O	■			■	■			■						■	■		RB
Adefarati et al. (2019)	O	■			■				■					■		■	■	MH
Aziz et al. (2019)	O	■			■				■					■		■		RB, H
García-Triviño et al. (2016)	O	■			■				■				■			■	■	MH
Marzband et al. (2016)	O	■				■			■						■	■		MH
Marzband et al. (2017)	O	■				■			■						■	■	■	MP
González-Briones et al. (2018)	O	■						■							■			RB
Luo et al. (2020)	O	■							■				■	■	■	■	■	MH
Shukhobodskiy and Colantuono (2020); Ortiz et al. (2021)	O		■			■			■			■		■	■	■	■	RB
Auñón-Hidalgo et al. (2021)	O					■	■		■			■		■	■	■		RB
Georgiou et al. (2020a)	O		■		■	■			■						■	■		MP
Georgiou et al. (2020b)	O		■		■	■			■						■	■		MP,MH
Zhang et al. (2012)	O	■	■		■	■			■						■	■		MCDA
		39	**27**	**2**	**18**	**20**	**5**	**3**	**38**	**2**	**2**	**5**	**6**	**18**	**28**	**31**	**14**	

analyzing different types of renewable energy infrastructures. Although our article focuses on the operational phase (optimizing energy storage over time), our review evidences that optimization also plays a key role at the design phase.

Regarding the articles at the operational (O) phase, most of the literature focuses on optimizing charging/discharging cycles of the energy storage systems to shift the consumption from peak to off-peak hours. As evidenced in Table 1, all the reviewed articles adopt a multi-objective optimization model, aiming at first – *in 85% of the reviewed articles* – reducing the electricity bill, second – *54%* – at reducing GHGE, third – *46%* – at improving sustainability aspects (e.g., extending the battery lifespan) and/or grid interdependency, while peak shaving and fuel reduction have been considered infrequently in the reviewed papers. The reason for this is twofold: (i) fuel reduction and peak shaving are often formulated as overarching objectives when there is no connexion

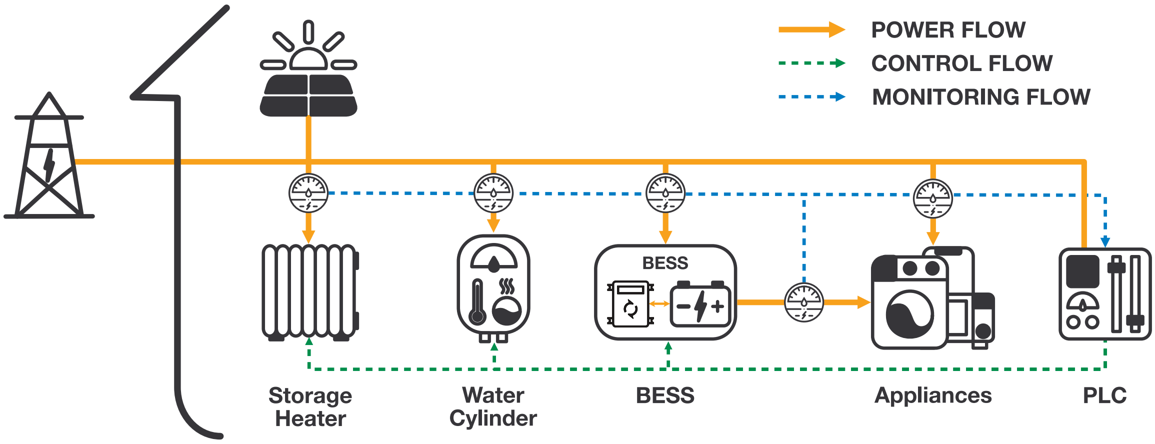

Figure 3: Overview of the RED WoLF's hardware architecture, along with the underlying power, data monitoring and control flows

to the electrical grid; and (ii) there are partly tackled implicitly when addressing the GHGE reduction and bill reduction problems (fuel reduction being mainly linked to GHGE and peak shaving to financial costs).. From an energy production and storage viewpoint, a significant proportion of the reviewed articles – *65%* – consider a combination of electrical grid, PV and BESS technologies, which can be explained by the fact that it is often the most economical configuration, as analyzed in (Murty and Kumar, 2020). Another interesting point is that a couple of approaches propose to combine different types of storage such as BESS and EV (Mahmud et al., 2018), BESS and hydrogen storage (Bhayo et al., 2020), or still BESS and thermal storage (e.g., water cylinder) (Terlouw et al., 2019b), which provides additional flexibility for energy management. Looking at the optimization techniques used for problem-solving, most of the approaches – *in 73% of the reviewed articles* – rely on optimization solvers or heuristic algorithms, which require a certain amount of time to find optimal solutions, often growing exponentially along with the increase of constraints and variables. This constitutes a serious impediment for the development of Edge Computing solutions in the energy sector, as thoroughly discussed by Feng et al. (2021).

Given the lack of approaches combining different types of storage systems, and the fact that most of them are computationally intensive, a new hybrid storage system for GHGE reduction in residential houses/dwellings is being developed by the Interreg NWE RED WoLF consortium, as originally presented in (Shukhobodskiy and Colantuono, 2020). Section 3 recalls the infrastructure and logic underlying RED WoLF, but also proposes an extension of the LP-based algorithm introduced by Olivieri and McConky (2020) with the aim to integrate PV into the model.

3. GHGE reduction systems

The hybrid-energy storage strategy proposed in RED WoLF is detailed in section 3.1. The extension of Olivieri's model is then presented in section 3.2.

3.1. RED WoLF optimization system

Figure 3 gives an overview of the hardware, electrical and communication architecture underlying the RED WoLF system introduced in (Shukhobodskiy and Colantuono, 2020) and further in (Ortiz et al., 2021), highlighting the power flow, monitoring flow (i.e., monitored devices) and control flow (controllable devices from the algorithm). As a first category of equipment, home appliances comprise all devices that consume electrical power and do not have any storage capability (e.g., TV, oven, light, *etc.*). It should be highlighted that, as of today, RED WoLF does not consider shiftable loads as an additional flexibility resource. From an energy supply perspective, RED WoLF considers two electrical power sources to supply the home appliances, namely (i) the national electrical grid, which is a non-renewable energy source as it has a carbon intensity, and (ii) a PV array, which is a renewable (non-polluting) source. In terms of flexible energy-storage devices, RED WoLF proposes a hybrid-energy storage system, combining electrochemical and thermal storage systems, as illustrated in Figure 3 (BESS, water cylinder and storage heaters). Finally, from a control viewpoint, the RED WoLF algorithm is executed in a PLC (see Figure 3), generating commands at different times to either store or draw a certain amount of power in/from the above described hybrid-energy storage system.

Based on the hardware constituents, several data are collected for use by the RED WoLF algorithm. These data can be categorized in three classes:

Table 2: Variables used in the RED WoLF optimization system

	Class	Variable	Units	Description
Input & Internal Variables	Real-time	A_{cur}	kW	Appliances present consumption
	Real-time	CO_{2cur}	gCO_2/kWh	Grid present CO_2 load
	Real-time	PV_{cur}	kW	PV present production
	Real-time	B_{lev}	kWh	Battery state of charge
	Real-time	C_{lev}	kWh	Cylinder state of charge
	Real-time	H_{lev}	kWh	Storage heater state of charge
	Predicted	A_{pre}	kW	Appliances predicted consumption
	Predicted	PV_{pre}	kW	PV predicted production
	Predicted	CO_{2pre}	gCO_2/kWh	Grid predicted CO_2 load
	Predicted	D_{ED}	kWh	Appliances predicted consumption until the end of the day
	Predicted	G_{PU}	kW	Grid predicted available mean drawable power
	Static	B_C	kWh	Battery capacity
	Static	B_{Imax}	kW	Battery maximum admissible power
	Static	C_{Imax}	kW	Cylinder maximum admissible power
	Static	C_{set}	kWh	Cylinder setpoint
	Static	D_{Imax}	kW	Grid power drawing limit (set by utility provider)
	Static	H_{Imax}	kW	Storage heater maximum admissible power
	Static	H_{set}	kWh	Storage heater setpoint
	N/A	C_{dem}	kW	Cylinder present power demand
	N/A	B_{dem}	kW	Battery present power demand
	N/A	$D_{ImaxAPV}$	kW	Grid and PV power available for HSS
	N/A	H_{dem}	kW	Storage heater present power demand
	N/A	P_{bal}	kW	Remaining power after supplying appliances and HSS
	N/A	CO_{2thr}	gCO_2/kWh	Control CO_2 threshold
	N/A	T_I	min	Smallest time to supply HSS considering appliances
Output Var.	Real-time	B_{con}	kW	Power to be drawn from the battery
	Real-time	B_{inj}	kW	Power to be stored in the battery
	Real-time	C_{cur}	kW	Power to be stored in the water cylinder
	Real-time	G_{con}	kW	Power to be drawn from the grid
	Real-time	G_{inj}	kW	Power to be injected to the grid
	Real-time	H_{cur}	kW	Power to be stored in the storage heater

i. *Static parameter values:* referring to fixed parameters such as manufacturers' data (e.g., maximum battery capacity);
ii. *Real-time data values:* referring to live data monitored at the hardware layer (e.g., data coming from smart meters, sensors in the battery, *etc.*);
iii. *Predicted data values:* referring to predicted data such as predicted grid carbon intensities, predicted PV generation and house consumption.

Table 2 (column denoted by class) reports what system variables belong to what class. It should be noted that some system parameters are both predicted (using ML) and monitored in real-time (e.g., via sensors), such as house appliance demand (respectively denoted by A_{pre} and A_{cur}), the output power produced by PV (PV_{pre}, PV_{cur}), or the grid carbon intensities (CO_{2cur}, CO_{2pre}). Based on the input data, the RED WoLF algorithm follows a two-step approach. First, a CO_2 threshold applied on the (predicted) grid intensity signal is computed, which identifies when it is optimal to draw energy from the grid to meet – *at minimum* – the house demand. Based on this threshold, a rule-based strategy is applied to decide the charging/discharging actions to be executed. These two steps are further described in the following paragraphs.

To compute the CO_2 threshold, the average available electrical power to supply the thermal storage system (G_{PU}), the energy required to reach the setpoint until the end of the day (D_{ED}), the heater and cylinder power demands (H_{dem} and C_{dem}) must be computed, as respectively given from Eq. (1) to (4).

$$G_{PU} = D_{Imax} - \int_t^T \frac{A_{pre}(t)}{(T-t)} dt - B_{Imax} \tag{1}$$

$$D_{ED} = \int_t^T \frac{A_{pre}(t)}{60} dt + \sum_{i=H,C} (i_{dem} - i_{lev}) \tag{2}$$

$$H_{dem} = H_{Imax} \times Heavi(H_{set} - H_{lev}) \tag{3}$$

$$C_{dem} = C_{Imax} \times Heavi(C_{set} - C_{lev}) \tag{4}$$

Several system constraints and state variables are

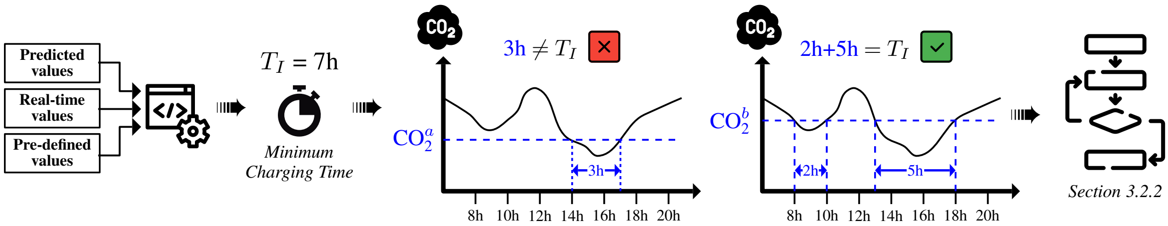

Figure 4: RED WoLF's CO_2 threshold computation example

used in this respect, such as the maximum charging power of the battery, cylinder and heater (respectively denoted by B_{Imax}, H_{Imax}, C_{Imax}), the maximum power drawable from the grid (D_{Imax}), or still the current level of charge of the heater and cylinder (H_{lev} and C_{lev}). Note that the Heaviside step function ($Heavi$) is defined as `True` (1) if the input is greater than 0, `False` (0) otherwise.

The minimum time length (T_I) to charge equipment is further computed from D_ED, G_{PU}, H_{dem} and C_{dem}, as given in Eq. (5).

$$T_I = \max\left(\frac{C_{dem} - C_{lev}}{C_{Imax}}, \frac{H_{dem} - H_{lev}}{H_{Imax}}, \frac{D_{ED}}{G_{PU}}\right) \tag{5}$$

The CO_2 threshold (CO_{2thr}), which identifies the best intervals for drawing electricity from the grid, is then computed using Eq. (7), $CO_{2preSort}$ referring to the CO_2 prediction vector sorted in ascending order, as given in Eq. (6).

$$CO_{2preSort} = sort(CO_{2pre}) \tag{6}$$

The ceil function used in Eq. (7) allows for getting an integer value, which represents the drawing time (in minutes) that is used as index in the sorted CO_2 vector to determine the CO_2 threshold.

$$CO_{2thr} = CO_{2preSort}(\lceil T_I \rceil) \tag{7}$$

Figure 4 illustrates the output when applying the above equations. Assuming a T_I equals to $7h$, the threshold that meets this charging duration should be identified. The first threshold example (denoted by CO_2^a in Figure 4) does not meet this requirement, while the second threshold (CO_2^b) does, resulting in two "low CO_2 periods": $[8am; 10am]$ and $[2pm; 6pm]$. Based on the computed threshold, a specific rule-based logic is applied, which is detailed in the form of a flowchart in Figure 5 using the UML activity diagram formalism. This flowchart shows that two parts are run in parallel. On the first part (see frame denoted by "CO_2 threshold computation" in Figure 5), the steps refer to the reading of sensor data needed to compute the CO_2 threshold (CO_{2thr}). Such data is either locally accessed (e.g., state of charge of the battery) or remotely (e.g., appliance consumption forecasts or grid carbon intensity forecasts that

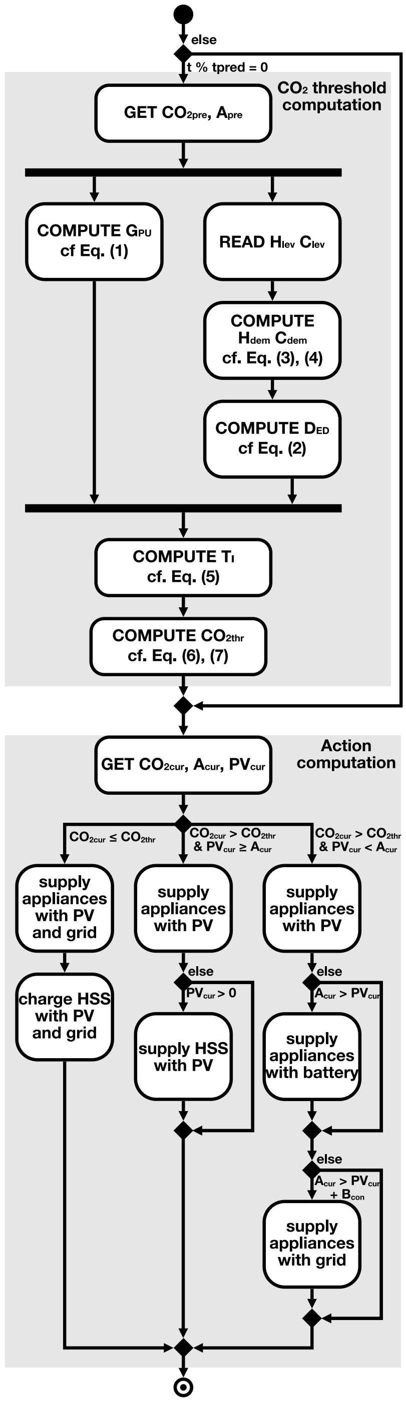

Figure 5: Overall RED WoLF logic

Table 3: Variables used in the Olivieri's optimization system (Olivieri and McConky, 2020)

	Class	Var.	Unit	Description
Input & Internal Variables	Predicted	d_i	kW	Power required to supply appliances over the time interval i
	Predicted	M_i	gCO_2/kWh	Grid CO_2 load over the time interval i
	Predicted	pv_i	kW	Power provided by PV over the time interval $_i$
	Real-time	Cap	kWh	BESS max capacity
	N/A	ppv_i	kW	Power from PV used by appliances over the time interval i
	N/A	bpv_i	kW	Power from PV injected to BESS over the time interval i
	N/A	gpv_i	kW	Power from PV sent back to grid over the time interval i
	N/A	$CO2_i$	gCO_2	CO_2 emitted over the time interval i
	N/A	SOC_i	kWh	BESS state of charge read over the time interval i
	N/A	I	hrs	Length of each time interval
	N/A	T	N/A	Set of discrete time intervals
	N/A	inef	%	Inefficiency factor (0 to 1)
Out.	N/A	pc_i	kW	Power charged in BESS over interval i
	N/A	pd_i	kW	Power discharged from BESS over i

are computed at the Cloud level). On the second part (see frame denoted by "Actions computation" in Figure 5), the steps refer to the decisions about the actions to be executed in terms of energy storage and release depending on the threshold value (CO_{2thr}), namely:

1. if $CO_{2cur} < CO_{2thr}$, appliances and the hybrid-energy storage system are powered by the grid and PV array;
2. if $CO_{2cur} > CO_{2thr}$ but PV is sufficient, appliances are powered through PV and extra-power (if any) is used to load the hybrid-energy storage system;
3. if $CO_{2cur} > CO_{2thr}$ and PV is insufficient, appliances are powered through PV; if not sufficient, through battery; if not yet sufficient, then through the grid.

It should be noted that the RED WoLF algorithm is inspired by the ARIMA (Autoregressive Integrated Moving Average) model (Siami-Namini et al., 2018), which in our case (considering the input data of our problem) adds non-linearity and other levels of complexity to the system. This is due to RED WoLF algorithm takes as the input the prediction values and current state of storage reservoirs, however the execution is done on current physical state of the system.

3.2. Olivieri's optimization system

OIivieri's optimization model considers the infrastructure detailed in Figure 6, the algorithm being run on a smart meter that controls the battery (Olivieri and McConky, 2020). The model uses a LP solver to reduce electricity bill, carbon emission, or both simultaneously. For a fair comparison with RED WoLF, only the model proposed for carbon emission reduction is considered in this study. This model is detailed through Eq. (8) to (17), which minimizes the

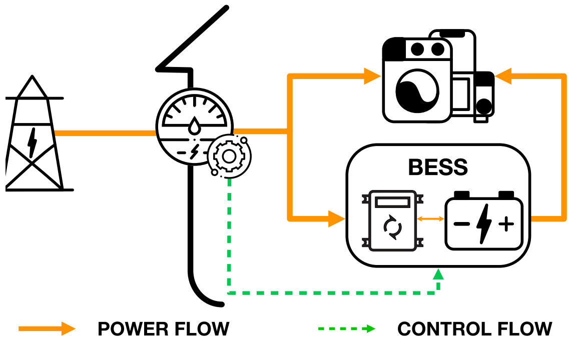

Figure 6: Olivieri's hardware architecture

CO_2 emissions produced to meet the household's energy demand during a time interval denoted by i.

$$\min Emissions = \sum_{i \in T} CO2_i \quad (8)$$

subject to

$$CO2_i = (d_i + pc_i - pd_i - \boldsymbol{ppv_i}) \cdot I \cdot M_i, \forall i \in T \quad (9)$$

$$pc_i \geq 0, \forall i \in T \quad (10)$$

$$pd_i \geq 0, \forall i \in T \quad (11)$$

$$(pc_i + \boldsymbol{bpv_i}) \leq Cap/2.7, \forall i \in T \quad (12)$$

$$SOC_i = \sum_{t=0}^{i} (pc_t + \boldsymbol{bpv_i}) \cdot inef \cdot I - \sum_{t=0}^{i} pd_t \cdot I, \forall i \in T \quad (13)$$

$$SOC_i \geq 0, \forall i \in T \quad (14)$$

$$SOC_i \leq Cap, \forall i \in T \quad (15)$$

$$\boldsymbol{gpv_i + ppv_i + bpv_i = pv_i, \forall i \in T} \quad (16)$$

$$\boldsymbol{gpv_i,\ ppv_i,\ bpv_i \geq 0, \forall i \in T} \quad (17)$$

CO_2 emissions are computed using Eq. 9, while

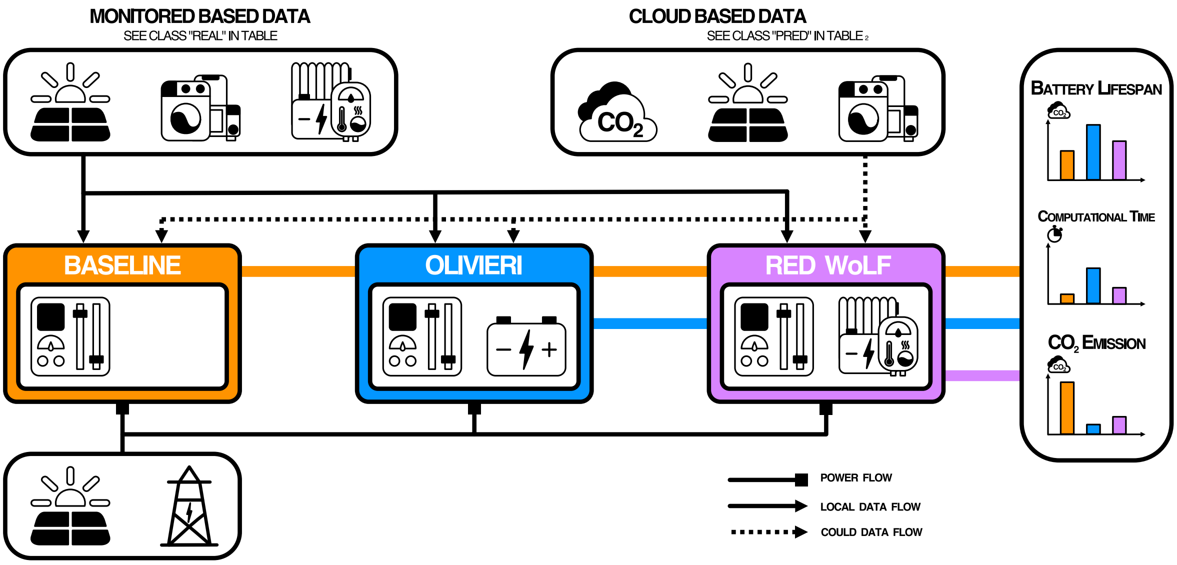

Figure 7: Comparison Infrastructure

Eq. (10) and (11) define the BESS charging and discharging constraints. Eq (12) represents the BESS maximum capacity to store energy, while the BESS state of charge (SOC) is computed using Eq. (13) to (15). Olivieri's model was slightly adapted to integrate the PV system to the infrastructure[2] for fair comparison with RED WoLF. Please note that the variables highlighted in **bold** in Eq. (8)to (17) represent the **extensions** of Olivieri's model in order to integrate the solar production into the optimization model, which was not proposed in the initial model; all variables being summarized in Table 3.

The complexity of Olivieri's model is given through Table 4, which provides information related to decision variables and constraints for different model sizes, which all consider 7 decision variables and 11 constraints per time period, as well as a time period length of 1 min. Furthermore, Pyomo modeling language with GLPK solver was used under the following configuration: 2,3 GHz Intel Core i7 quad core with 32 Go RAM

4. Experimental evaluation

To evaluate the performance of RED WoLF, three scenarios are defined and compared, as illustrated in Figure 7. In the first scenario (denoted by "Baseline" in Figure 7), the carbon footprint in terms of kg equivalent CO_2 emissions (denoted by *kg eq.* CO_2 in the rest of the paper) is computed for a given residential house and a given energy consumption demand. As energy supply sources, the considered house has a PV installation and is connected to the grid, but it does not have any storage system nor optimization logic. In the second scenario (denoted by "Olivieri"), Olivieri's optimization algorithm is implemented and compared against the baseline scenario. In the third scenario (denoted by "RED WoLF"), the RED WoLF hybrid-energy storage system is implemented and compared against the Baseline and Olivieri scenarios. Let us stress the fact that the comparison between RED WoLF or Olivieri's algorithms is established on a fair basis, as the two algorithms consider similar input data (PV energy production, energy storage system connected to a battery, house electricity demand, grid carbon intensity) and seek to optimize the same criterion (i.e., carbon emission reduction). The other results that will be compared in the rest of the study, such as electricity bills or battery lifespan correspond to side effects on other parameters.

Section 4.1 presents the datasets used as inputs of the conducted experimental evaluation. Section 4.2 presents the performance comparison analysis of the three scenarios.

Table 4: Complexity of Olivieri's model related to decision variables and constraints for different model sizes (7 decision variables, 11 constraints per time period, period length of 1 min).

Horizon (hours)	Total Time Periods	Number of decision variables	Number of constraints
4	240	1680	2640
8	480	3360	5280
12	720	5040	7920
24	1440	10080	15840
36	2160	15120	23760
48	2880	20160	31680
60	3600	25200	39600
72	4320	30240	47520

[2]The average electricity consumption of the thermal heating and hot water are computed (respectively being equal to 1.04 kW + 0,167 kW) and added to the total house demand.

Table 5: Datasets used as experimental inputs

Dataset	Loc.	Name	Period	URL
House demand	UK	UKDALE	Oct.	(UKDALE, 2015)
	FR	IHEPCDS	Oct.	(IHEPCDS, 2010)
PV production	UK	N/A	Oct.	(NREL, 2020)
	FR	N/A	Oct.	(Eur, 2020)
Grid carbon intensity	UK	N/A	Oct.	(CIA, 2020)
	FR	N/A	Oct.	(RTE, 2022)
Energy price	UK	N/A	N/A	(Statista, 2021)
	FR	N/A	N/A	

4.1. Experimental setup

As illustrated in Figure 7, the three scenarios are going to be compared on the basis of three performance indicators, namely *(i) CO_2 emissions*: CO_2 equivalent greenhouse gas emissions produced for supplying house electrical power demand in kg eq. CO_2; *(ii) Computational time*: time needed to generate the recommended set of commands to be executed; *(iii) Battery lifespan*: amount of time a battery lasts until it needs to be replaced. In terms of input data, four data sources have been considered:

1. *Home consumption:* the state-of-the-art UK-DALE (UK Domestic Appliance-Level Electricity) and IHEPCDS (Individual Household Electric Power Consumption Data Set) datasets have been considered in this study, which provide real house consumption behaviors from houses located in UK and France respectively (Monacchi et al., 2014) (see Table 5 for further details). The reason for considering these two datasets is twofold: (i) as of the pilots (currently being setting up) of the RED WoLF project are located in these two countries; (ii) these two countries have different ways of generating electricity (nuclear in France, natural gas in UK), which have direct impact on the grid's carbon intensity. This study considers the October month;
2. *PV production:* to the best of our knowledge, there is no platform in France providing real-time PV production, while in UK the NREL (National Renewable Energy Laboratory) web platform makes available both historical and predicted PV datasets. A simulator developed by the European Commission (*cf.*, Table 5) nonetheless shows that there is a difference of 15.4% between UK and France (in favor of France). On this basis, the PV production dataset in UK (obtained via the NREL platform) was increased by 15.4% for the French experiments;
3. *Grid carbon intensity:* two distinct web platforms making carbon intensity available for France and UK were used, namely RTE for France and Carbon Intensity for UK (*cf.*, Table 5).

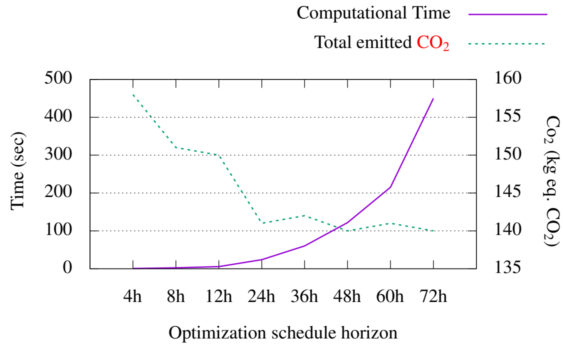

Figure 8: Overview of the Computational Time and associated performance in terms of total emitted CO_2 with Olivieri's system

For a fair and consistent comparison between scenarios, the energy demands of the Baseline and Olivieri models have been slightly adjusted to include the power used for space and water heating in the RED WoLF scenario. It should also be noted that the time interval *i* in Olivieri's algorithm has been set to 1 min in our experiments.

4.2. Experimental results

In this section, the three scenarios/algorithms (Baseline *vs.* Olivieri *vs.* RED WoLF) are compared over a 1-month period (October). However, before doing so, a pre-study is conducted in section 4.2.1 to determine the prediction horizon length to run the algorithms. Then, a comparison of the Olivieri and RED WoLF algorithms over three specific days is then conducted in section 4.2.2 to understand the behavior of each algorithm with respect to the different inputs, before conducting the 1-month comparison analysis in section 4.2.3. Finally, in section 4.2.4, we analyze to what extent a battery with different characteristics (different capacities, maximum power intake) may impact on the algorithm performance, along with what would be the best configuration (technology) to be selected.

4.2.1. Prediction horizon length determination

Due to the low complexity in computing the threshold in RED WoLF, the scheduling process is almost instantaneous ($<$ 1 ms), as thoroughly analyzed in (Shukhobodskiy et al., 2021). In opposition, Olivieri's algorithm processing time varies exponentially according to the length of the prediction horizon. Figure 8 provides clear evidence of such an exponential behavior, showing that the longer the prediction horizon length (x-axis), the more exponential Olivieri's algorithm processing time (y-axis). Indeed, optimizing the energy storage and release with a 4h-prediction time window requires less than one second, while this processing time reaches 6h with a 72h-prediction time window (*cf.*, Figure 8). As a complementary information, the total CO_2 emitted

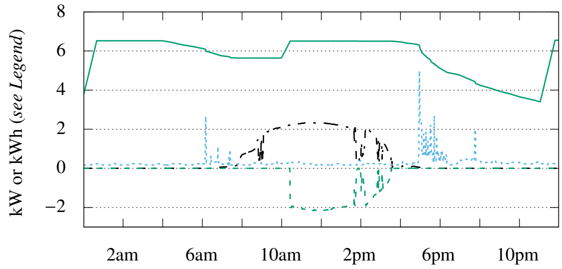

(a) RED WoLF system in UK scenario

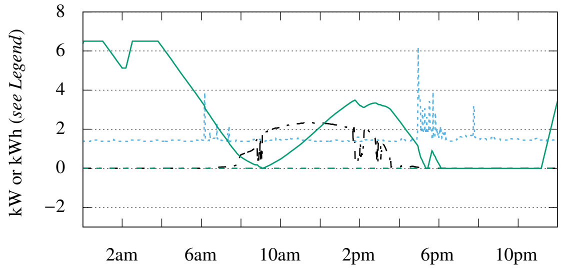

(b) Olivieri system in UK scenario

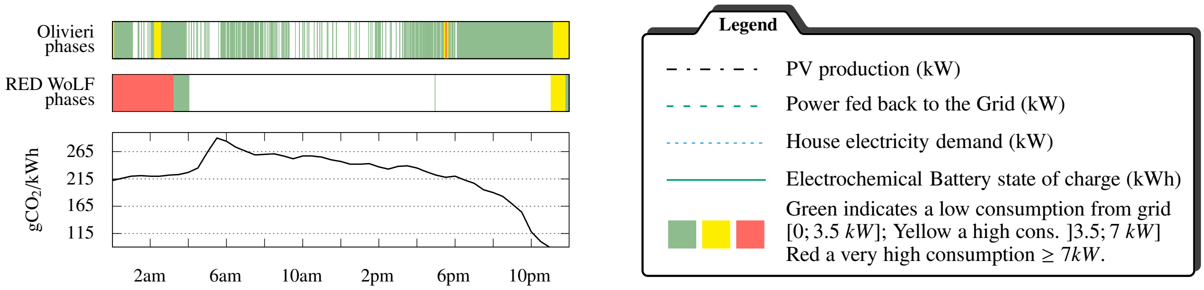

(c) Grid carbon intensity evolution, along with a representation of when and what proportion of power the RED WoLF and Olivieri systems should be drawn from the electrical grid. In this scenario, RED WoLF draws power from the grid in an intensive manner from 0:00 (midnight) to ≈3:30am (i.e., drawing power in a range of $\geq 7kW$, as indicated in the Legend frame), while Olivieri's algorithm generates charging orders all over the day (i.e., in a continuous manner) in a less intensive manner (in a range of $[0; 3.5kW[$). To understand the impact of such behavior on the battery state of charge, the reader shall refer to Figures 9(a) and 9(b).

Figure 9: October 3rd - One day analysis of how RED WoLF and Olivieri systems behave with respect to the different inputs

with the Olivieri's algorithm over the October month is depicted in Figure 8, showing that beyond a 24h-prediction time window, the optimization does not lead to better performance. As a consequence, a 24h-prediction time window is chosen for running the experiments conducted in the rest of the paper, bearing in mind that in this configuration Olivieri requires $\approx$ 25 min for generating the optimal solution against < 1 *ms* with RED WoLF.

4.2.2. Daily analysis

Before presenting the monthly comparison analysis, which is the subject of section 4.2.3, we suggest to analyze how RED WoLF and Olivieri algorithms behave with respect to the system inputs considering three specific days. Let us note that, in the conducted experiments, the battery capacity for both algorithms is 6.5 kWh and the maximum intake/outtake power is 4.2 kW. Furthermore, two assumptions differ between RED WoLF and Olivieri: *(i) maximum grid intake:* RED WoLF defines a constraint defining the maximum power that can be drawn from the grid by the sum of house consumption minus the power generated by the PV system. This limit is fixed by the energy provider and set to 9 kW. Olivieri's algorithm does not include such a constraint; *(ii) Thermal charging using battery:* In Olivieri, space heating and hot water needs are considered as appliances and therefore could be supplied by the battery, unlike RED WoLF where thermal reservoir must be supplied by the grid or PV unit sources (this constraint has been added to avoid energy losses during energy conversion). This is why in Figure 9(b) the appliance demand in Olivieri is greater than in RED WoLF (*cf.*, Figure 9(a)).

October 3rd: Power exchanges occuring between the grid, appliances, PV arrays and the hybrid energy storage system when using the RED WoLF and Olivieri strategies are plotted in Figures 9(a) and 9(b) respectively. A complementary plot of the amount of grid carbon intensity over that day is given in Figure 9(c), along with the periods when RED WoLF and Olivieri algorithms draw power from the grid (a color code being used to indicate the intensity of consumption, as detailed in the "Legend" of Figure 9). A first reading of the graphs shows a different behavior of the battery management system. In RED WoLF, the battery has a constantly high level of charge (see Figure 9(a)), whereas the battery level is highly variable when using Olivieri's algorithm, going from fully charged to empty several times over that day (see Figure 9(b)). It can also be noted that the battery is mainly charged by the local PV production in both cases, which can be partly explained by the grid carbon intensity that is consistently high that day (above 200g eq. CO_2 per kWh). From a more detailed examination of those plots, it can be noted that:

- during the night, batteries are fully charged in both algorithms as the grid carbon intensity is

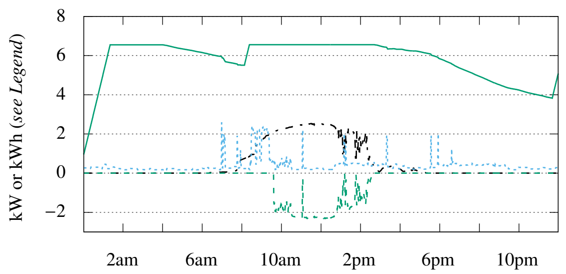

(a) RED WoLF system in UK scenario

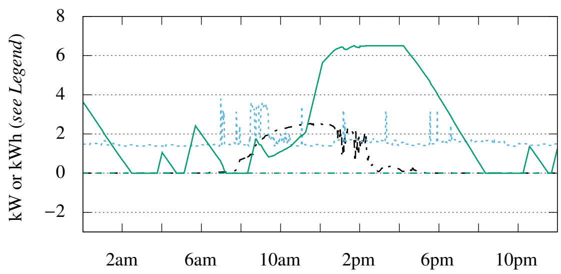

(b) Olivieri system in UK scenario

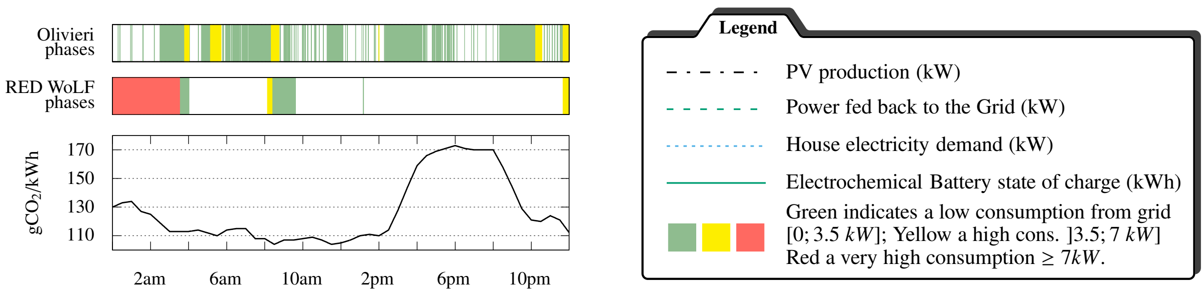

(c) Grid carbon intensity evolution, along with a representation of when RED WoLF and Olivieri systems draw power from the electrical grid

Figure 10: October 6th - One day analysis of how RED WoLF and Olivieri systems behave with respect to the different inputs

lower – *even if it remains high* – than the rest of the day. Figure 9(b) shows that RED WoLF draws power from the grid in an intensive manner to charge all storage systems (i.e., battery, water cylinder and storage heaters);

- in the morning (likely because residents get up), batteries are discharged in both models. In Olivieri, the battery is almost completely discharged, which is mostly due to the fact that it is not possible to store energy in the heater and/or water cylinder, unlike RED WoLF in which both storage systems have been charged during the night (at the same time as the battery);

- batteries are then charged during sunshine hours. However, as the battery's SOC in RED WoLF is always high, the battery quickly becomes full and solar energy produced locally is redirected to the grid. For that day 62% of the PV production in RED WoLF (eq. to $8,4$ kWh) is fed back to the grid, while all the PV production is adsorbed by the battery with Olivieri;

- at the end of the day, when the house electricity demand increases, the RED WoLF system is self-sufficient (operating solely on its battery), while Olivieri's schedule draws power from the grid. In this respect, RED WoLF, which keeps a high battery's SOC, has an advantage in the event of a grid failure or disconnection;

Let's remind ourselves that the primary objective of RED WoLF and Olivieri is to reduce GHGE. For this specific day (Oct. 3rd), the latter (Olivieri) provides significantly lower emissions than RED WoLF as it makes use of the whole PV production, unlike RED WoLF that exports part of that production to the grid. In numerical terms, Olivieri emits half as much GHGE (3.2 kg eq. CO_2) than RED WoLF (6.9 kg eq. CO_2). Another aspect that can be analyzed is the wear and tear of the battery as a result of charge/discharge cycles, which has a direct impact on the battery lifetime (Karamov and Suslov, 2021). Even if the maximization of the battery lifespan is not defined as an objective in RED WoLF or Olivieri, it is interesting to be analyzed, as replacing a battery has a threefold environmental impact: (i) producing new batteries results in depleting the earth's resources; (ii) managing battery disposal today is a concern; (iii) increasing costs due to the battery purchase leads to social concerns. Overall, Olivieri results in twice more charging/discharging phases[3] (10 in total) than RED WoLF (5 in total).

October 6th: A second day is analyzed in Figure 10 in order to see whether a similar energy management behavior is observed. It can be first observed that unlike Oct. 3rd, the grid carbon intensity signal strongly varies over time (see Figure 10(c)), although it is globally cleaner than the signal of Oct. 3rd (see Figure 9(c)). Overall, the behavior of the house when

[3] A distinction between charge/discharge phases and cycles is made. One cycle is when we have charged or discharged an amount that equals 100% of the battery's capacity, but not necessarily all from one charge, while a phase refers to cases where we switch from charging to discharging command, or *vice-versa*.

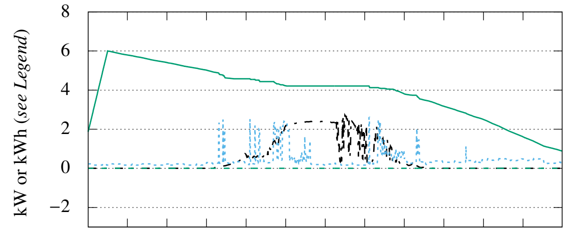

(a) RED WoLF system in UK scenario

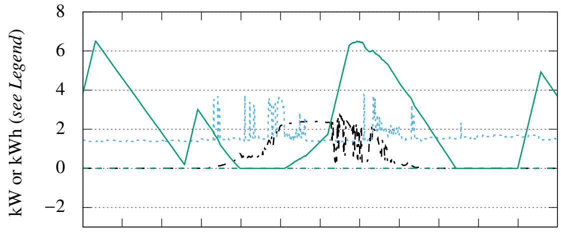

(b) Olivieri system in UK scenario

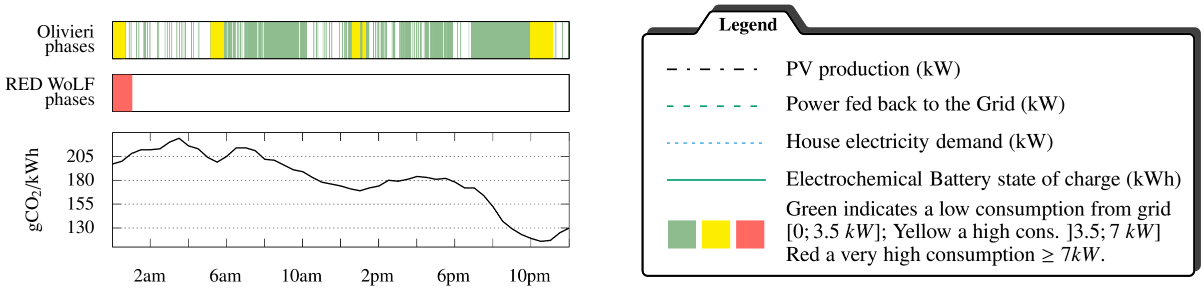

(c) Grid carbon intensity evolution, along with a representation of when RED WoLF and Olivieri systems draw power from the electrical grid

Figure 11: October 5th - One day analysis of how RED WoLF and Olivieri systems behave with respect to the different inputs

using RED WoLF and Olivieri (see Figures 10(a) and 10(b)) is quite similar to the one analyzed in Oct. 3rd (battery's SOC remaining high and part of the PV production – *8,7 kWh* – being fed back to the grid). One difference lies in the fact that RED WoLF is no longer self-sufficient in the morning (from 8am to 10am), as it draws power from the grid to first charge the battery and then power the appliances (*cf.* Figure 10(c)). The reason for this is twofold: (i) the carbon grid intensity is low during that period (≈ 100 g eq. CO_2), and (ii) RED WoLF predicts that the intensity will significantly increase within the following 12h. With Olivieri, the charging pattern differs from Oct. 3rd; the battery starts with a half SOC, while it was full in Oct. 3rd. In a similar way as RED WoLF, Olivieri's algorithm takes the opportunity to both satisfy the house electricity demand and charge the battery when the carbon intensity is low (until 4 pm). From this time onwards, the battery in Olivieri becomes the only source of supply until 8 pm (when the grid electricity becomes cleaner again). As on Oct. 3rd, Olivieri's system uses all the PV production, while RED WoLF re-injects part of this production into the grid. Regarding now the number of charge/discharge phases, 5 phases are identified in RED WoLF against 12 in Olivieri, which is mostly due to the greater variability in the carbon intensity.

Day 5 of October: The grid carbon intensity of this third day is given in Figure 11(c), which is relatively high at the beginning of the day, and then progressively decreases. Looking at Figures 11(a) and 11(b), it can be observed that the RED WoLF is charging the storage units straight at the beginning of the day, which, combined with the PV production, is sufficient to meet the house electricity demand without consuming power from the grid, nor exporting surplus electricity. With Olivieri, several periods of battery charging/discharging can be observed. In total, 2 charging/discharging cycles are identified with RED WoLF, against 8 with Olivieri, where the total carbon emission for that day is estimated to 4.1kg eq. CO_2 for Olivieri, against 1.8kg eq. CO_2 for RED WoLF. The main reason leading to this result is the the non support (in Olivieri) of a hybrid-storage system (i.e., considering the water cylinder and storage heaters as storage units).

4.2.3. One Month analysis

Figures 12(a) and 12(b) provide, for each day in October, the difference in CO_2 between the RED WoLF and Olivieri algorithms for France and UK datasets respectively; a positive value indicating that RED WoLF outperforms Olivieri, and *vice-versa*. It can be observed in Figure 12(a) that there is no clear outperforming algorithm and the difference in results is small (0.3 kg eq. CO_2 at most). This difference can be explained by the fact that France uses nuclear power for most of its electricity, which has a very low GHGE rate compared with UK. In the case of UK (see Figure 12(b)), Olivieri's algorithm outperforms RED WoLF in ≈ 60% of the time. Nevertheless, in order to gain a full and complete comparison, other information such as the battery lifespan, the amount of energy redirected to the grid (ignored into account in Fig-

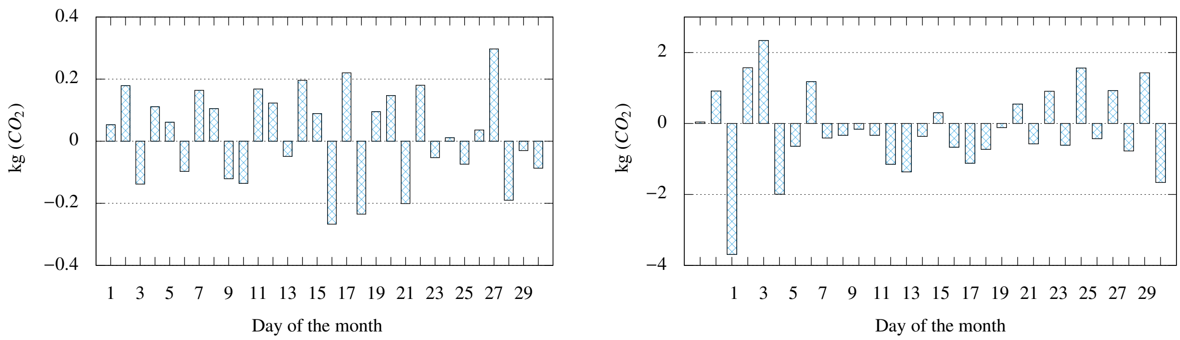

(a) RED WoLF *vs.* Olivieri (France)

(b) RED WoLF *vs.* Olivieri (UK)

Figure 12: RED WoLF *vs.* Olivieri: a positive value indicating that RED WoLF outperforms Olivieri and *vice-versa*.

Table 6: Summary of key results obtained with the Baseline, RED WoLF and Olivieri systems over the whole month of October

		kWh from Grid	Elec. bill (euros)	kg eq. CO_2 from Grid	Local PV usage (%)	PV to Grid (kWh)	Nb. of Cycles	Battery life-span (months)	Comput. Time
FR	Baseline	1454	257	N/A	100	N/A	N/A	N/A	N/A
	RED WoLF	1344	237	39	86	50.6	71	78	$< 1ms$
	Olivieri	1296	227	40	100	0	190	31	$25min$
UK	Baseline	1042	221	171	100	N/A	N/A	N/A	N/A
	RED WoLF	935	198	146	58	137.4	43	139	$< 1ms$
	Olivieri	806	142	140	100	0	133	45	$23min$

ure 12), or still the computational complexity of each algorithm. Table 6 provides such complementary information for both scenarios (France and UK).

Firstly, let us compare the results obtained with RED WoLF and Olivieri with the Baseline scenario (*cf.*, Figure 7). Table 6 reports that in both cases (France and UK), the monthly CO_2 emissions is reduced by 10% (France) and 30% (UK) when implementing RED WoLF's or Olivieri's system, with a slight advantage for the latter. However, as previously mentioned, this result does not take into consideration the PV electricity re-directed to the grid. Table 6 reports that Olivieri is consuming 100% of the local PV production, while RED WoLF consumes only 86% (France) and 58% (UK). Although it is preferable to consume locally the electricity (to avoid electricity losses during transmission), the results given and discussed in Figure 12 need to be put into perspective.

Secondly, looking at the electricity bills, Olivieri outperforms RED WoLF with a difference of more than 50€ in the UK scenario and 10€ in the French one. This can be explained by the fact that Olivieri consumes all the local PV production, unlike RED WoLF that re-injects part of the production to the grid, as previously discussed. Here again, some revenue could be generated in that case, which has not been taken into account in this study. Although the objective of reducing the electricity bill has not been defined as the prime objective in RED WoLF, nor in Olivieri (the focus being given to GHGE reduction), it can be noted that ecology considerations are not systemically in contradiction with financial ones.

Thirdly, the total number of charge/discharge cycles of the battery over the month is calculated using the definition of a cycle, which consists of accumulating the energy charged in the battery by dividing it by its maximum capacity (in this case the battery has a capacity of 6.5 kwh), the same calculation being done for the discharge. Summing up the charge and discharge cycles, the values reported in Table 6 are obtained. It can be noted that RED WoLF reduces by 60% (France) and 50% (UK) the number of cycles compared with Olivieri. Considering now the battery specification, which is expected to operate for a total of 6000 cycles, it can be concluded that the battery will likely need to be replaced after 3 to 4 years with Olivieri, against 7 to 12 years with RED WoLF.

Fourthly, it is important to remind ourselves that the RED WoLF's optimization is almost instantaneous (less than $1ms$), while Olivieri's optimization takes about 25 min. This is not negligible as it has an indirect impact on the overall system carbon footprint (the higher the algorithm complexity, the heavier the computational load). Furthermore, if we consider extending Olivieri's model to integrate other storage units such as storage heaters, water cylinder, or any other type of storage unit, this would result in an even larger complexity. Finally, with the advent of the Edge Computing, RED WoLF algorithm turns to be more appropriate than Olivieri to be deployed on devices that

Table 7: Total CO_2 emitted over the month of October using batteries of different capacities/sizes

		Bluetti		LG3.3		LG6.5		Tesla	
		CO_2 *kg eq.* CO_2	PV to Grid *kWh*	CO_2 *kg eq.* CO_2	PV to Grid *kWh*	CO_2 *kg eq.* CO_2	PV to Grid *kWh*	CO_2 *kg eq.* CO_2	PV to Grid *kWh*
FR	RED WoLF	42.13	140.16	40.50	138.47	39.48	137.41	37.70	137.73
	Olivieri	42.53	17.87	41.28	0.59	40.04	0	40.04	0
UK	RED WoLF	152.80	90.38	147.34	61.33	146.21	50.60	146.32	44.23
	Olivieri	157.57	12.96	148.57	3.08	140.79	0	128.35	0

have limited computational capabilities such as smart meters.

4.2.4. *Impact of different batteries on the optimization performance*

To study the impact of how a battery with different characteristics may impact on the algorithm performance, we consider four different technologies today available on the market, namely Bluetti, LG3.3, LG6.5 and Tesla, whose respective characteristics are summarized in Table 8 (battery capacity and maximum power intake). Table 7 reports the total CO_2 emission (in kg eq. CO_2) and power re-injected to the grid (in kWh) obtained when running the RED WoLF and Olivieri algorithms with these four batteries.

Table 8: Battery products (from the market) analyzed

	Bluetti	LG3.3	LG6.5	Tesla
B_{Imax} (kW)	1	3.3	4.2	7
B_C (kWh)	1.5	3.3	6.5	13.5

In the UK scenario, It can be noted that increasing the size and power intake of the battery leads to a significant reduction of CO_2 emission in Olivieri, which is not true for RED WoLF. The reason for this is highly correlated to the amount of energy re-injected into the grid, as Olivieri is better than RED WoLF in maximizing the consumption/storage of local PV production (*cf.*, PV to grid values in Table 8). Interestingly, RED WoLF outperforms Olivieri when using the smallest (Bluetti) battery, while the trend is reversed with the three other battery technologies. Overall, the LG3.3 is sufficient in RED WoLF, as larger batteries do not lead to a substantial improvement in CO_2 reduction, while the bigger the battery the better in Olivieri. This obviously has a financial impact.

In the FR scenario, RED WoLF always outperforms Olivieri, adding that the total CO_2 emission decreases along with the increase of the battery size, which does not apply for Olivieri. One reason for this lies in the RED WoLF logic that gives as much importance to low-carbon grid periods as local PV production, which may prove to be an effective strategy when the national grid is of low carbon, as is the case in France.

Overall, this study suggests that the choice of given strategy/algorithm and of a battery technology may depend on the country's strategic position in energy geopolitics.

5. Conclusion & Research implications

5.1. *A European willingness to primarily focus on GHGE reduction*

Climate change and the continuous and rapid rise in temperature are forcing international political bodies to focus on reducing GHGE to save the planet. The housing sector is heavily contributing to global warming. Gone are the days where everyone tries to find optimal solutions to reduce financial costs, whatever the environmental cost. This is in line with the commitments of the signatory countries of the Paris conventions (COP21), whose objective is to reduce carbon emissions from various human activities by 2030 (housing being one of the key focus).

The research conducted in this article – *which is part of the RED WoLF Interreg NWE project* – directly addresses the Interreg NWE's Low Carbon" Priority[4], which is why the proposed solution is an all-carbon optimisation, while being aware that other factors can have an impact. In other terms, the carbon aspect is considered as a restrictive objective, which is aligned with a political will of the EU (COP21).

5.2. *Comparison of two GHGE reduction models*

The current state-of-affairs reviewed in this paper brings evidence that most of today's energy management systems primarily focus on electricity bill reduction, placing GHGE reduction on the backburner, they rarely propose hybrid-energy storage optimization strategies, neither evaluate how the proposed strategy impacts on the computational complexity nor on the battery lifespan. The two last impacts are of particular importance with both the advent of Edge Computing in the energy sector (Feng et al., 2021) and the growing awareness of the the difficulty to

[4] Outline of the NWE's Low Carbon Priority available at: https://www.nweurope.eu/about-the-programme-2014-2020/the-themes/, last access June 1st 2022

manage and recycle renewable technologies such as batteries and PV modules (Nain and Kumar, 2022).

To progress this state-of-affairs, an innovative CO_2 threshold-based strategy currently being developed as part of a European project named RED WoLF (Rethink Electricity Distribution Without Load Following) has been proposed in our previous research work (Ortiz et al., 2021), which seeks to identify the best periods of the day to charge and discharge multiple types of storage units (incl., battery, storage heaters, water cylinder). In the present article, RED WoLF is evaluated and compared with a second strategy proposed by Olivieri and McConky (2020), which also aims at reducing GHGE but with a slightly different infrastructure (only considering a battery as flexible energy-storage) and algorithm designed based on Linear Programming (LP). The comparison study brings evidence that the two strategies (RED WoLF and Olivieri) contribute to significantly reduce GHGE compared to a solution without any optimization logic, although Olivieri has a slight advantage (11% of reduction with Olivieri against 8% with RED WoLF). However, as analyzed in this article, the behavior of the two algorithms is different in terms of charging/discharging periods, resulting in different *pros* and *cons* for the two strategies. Olivieri's algorithm has a more dynamic management of the batteries with a multitude of charging/discharging cycles over the days, which has the advantage of maximizing the consumption of local PV production, but, in comparison to RED WoLF, is less self-sufficient in the event of a power outage or of long periods of high grid carbon intensity. Such an aspect could eventually be of interest for distribution system operators during load shedding. RED WoLF also has the advantage of limiting the number of charging/discharging cycles compared with the Olivieri's algorithm, which contributes in extending the battery's lifespan (in average, 109 months with RED WoLF against 38 with Olivieri's model), which has a direct impact on the overall system cost and carbon footprint (i.e., reducing maintenance costs, battery replacement, *etc.*). Another *pros* of RED WoLF lies in the algorithmic complexity, which is very low compared to Olivieri (RED WoLF requiring less than a second to find an optimal solution, while Olivieri requires about 20 to 30min), and this conclusion would be the same with any other strategy using LP. This has a twofold consequence: (i) RED WoLF can be extended with additional objectives and constraints without causing extra computational burden; (ii) RED WoLF is lighter, resulting in a lower GHGE and making it more suitable to be deployed on edge devices.

Overall, our study does not allow to derive generic conclusions and findings, but still it brings interesting empirical evidence that two models designed on two distinct theories lead to very different behaviors and side effects (whether from a financial and battery lifespan perspective).

5.3. Further considerations in future research

It should be noted that both RED WoLF and Olivieri strategies imply the integration of PV arrays, battery and ICT technologies, which have a non negligible environmental impact considering the whole lifecycle of such technologies. The recent article of Sebestyén (2021) provides an interesting analysis in this regard, showing that in the case of wind, hydro-, geothermal, solar and biomass power plants falling ice, changes in the flow regime of rivers, noise, erosion caused by panels and the scale of harvesting, respectively, are the most critical environmental impacts.

From a research perspective, further studies and tools for Life Cycle Assessment (LCA) and Life Cycle Cost (LCC) should be developed to evaluate the overall sustainability of renewable energy systems/architectures, i.e. not only considering the operational phase, but also on the design phase (e.g., considering the quantity of available raw materials) and the recycling/disposal one. In this respect, forecasts about dynamics of raw materials (e.g., raw material reserves) released by *EIT RawMaterials*-like initiatives[5] could be considered and integrated to such analyses.

Acknowledgement

This work has been supported by the European Regional Development Fund and Interreg NWE, project RED WoLF, project number NWE847.

References

S. Baek, S. Kim, Potential effects of vacuum insulating glazing application for reducing greenhouse gas emission (ghge) from apartment buildings in the korean capital region, Energies 13 (2020) 2828.

M. Lazarus, H. van Asselt, Fossil fuel supply and climate policy: exploring the road less taken, Climatic Change 150 (2018) 1–13.

A. Ahmed, T. Ge, J. Peng, W.-C. Yan, B. T. Tee, S. You, Assessment of the renewable energy generation towards net-zero energy buildings: A review, Energy and Buildings (2021) 111755.

O. A. Al-Shahri, F. B. Ismail, M. A. Hannan, M. S. H. Lipu, A. Q. Al-Shetwi, R. A. Begum, N. F. O. Al-Muhsen, E. Soujeri, Solar photovoltaic energy optimization methods, challenges and issues: A comprehensive review, Journal of Cleaner Production 284 (2021) 125465.

M. A. Hannan, S. B. Wali, P. J. Ker, M. S. Abd Rahman, M. Mansor, V. K. Ramachandaramurthy, K. M. Muttaqi, T. M. I. Mahlia, Z. Y. Dong, Battery energy-storage system: A review of technologies, optimization objectives, constraints, approaches, and outstanding issues, Journal of Energy Storage 42 (2021) 103023.

A. A. Shukhobodskiy, G. Colantuono, Red wolf: Combining a battery and thermal energy reservoirs as a hybrid storage system, Applied Energy 274 (2020) 115209.

[5]https://eitrawmaterials.eu, last access June 1st 2022

P. Ortiz, S. Kubler, E. Rondeau, J.-P. Georges, G. Colantuono, A. A. Shukhobodskiy, Greenhouse gas emission reduction system in photovoltaic nanogrid with battery and thermal storage reservoirs, Journal of Cleaner Production 310 (2021) 127347.

M. Wiesheu, L. Rutešić, A. A. Shukhobodskiy, T. Pogarskaia, A. Zaitcev, G. Colantuono, Red wolf hybrid storage system: Adaptation of algorithm and analysis of performance in residential dwellings, Renewable Energy 179 (2021) 1036–1048.

M. S. Munir, S. F. Abedin, N. H. Tran, C. S. Hong, When edge computing meets microgrid: A deep reinforcement learning approach, IEEE Internet of Things Journal 6 (2019) 7360–7374.

Z. T. Olivieri, K. McConky, Optimization of residential battery energy storage system scheduling for cost and emissions reductions, Energy and Buildings 210 (2020) 109787.

Y. Saleem, N. Crespi, M. H. Rehmani, R. Copeland, Internet of things-aided smart grid: Technologies, architectures, applications, prototypes, and future research directions, IEEE Access 7 (2019) 62962–63003. doi:10.1109/ACCESS.2019.2913984.

D. Burmester, R. Rayudu, W. Seah, D. Akinyele, A review of nanogrid topologies and technologies, Renewable and Sustainable Energy Reviews 67 (2017) 760–775.

G. S. Georgiou, P. Christodoulides, S. A. Kalogirou, Real-time energy convex optimization, via electrical storage, in buildings–a review, Renewable energy 139 (2019) 1355–1365.

F. Tooryan, H. HassanzadehFard, E. R. Collins, S. Jin, B. Ramezani, Smart integration of renewable energy resources, electrical, and thermal energy storage in microgrid applications, Energy 212 (2020a) 118716.

F. Tooryan, H. HassanzadehFard, E. R. Collins, S. Jin, B. Ramezani, Optimization and energy management of distributed energy resources for a hybrid residential microgrid, Journal of Energy Storage 30 (2020b) 101556.

R. Das, Y. Wang, G. Putrus, R. Kotter, M. Marzband, B. Herteleer, J. Warmerdam, Multi-objective techno-economic-environmental optimisation of electric vehicle for energy services, Applied Energy 257 (2020) 113965.

A. Yazan M., A. Alaa M., E. Abo Eleyoun, E.-W. Amged S., A. Almoataz Y., U. Vadim, U. Ali Arshad, Optimal configuration and energy management scheme of an isolated micro-grid using cuckoo search optimization algorithm, Journal of the Franklin Institute 356 (2019) 4191–4214.

A. B. Awan, M. Zubair, G. A. S. Sidhu, A. R. Bhatti, A. G. Abo-Khalil, Performance analysis of various hybrid renewable energy systems using battery, hydrogen, and pumped hydro-based storage units, International Journal of Energy Research 43 (2019) 6296–6321.

M. A. Ashraf, Z. Liu, A. Alizadeh, S. Nojavan, K. Jermsittiparsert, D. Zhang, Designing an optimized configuration for a hybrid pv/diesel/battery energy system based on metaheuristics: A case study on gobi desert, Journal of Cleaner Production 270 (2020) 122467.

A. B. Awan, Performance analysis and optimization of a hybrid renewable energy system for sustainable neom city in saudi arabia, Journal of Renewable and Sustainable Energy 11 (2019) 025905.

F. Fodhil, A. Hamidat, O. Nadjemi, Potential, optimization and sensitivity analysis of photovoltaic-diesel-battery hybrid energy system for rural electrification in algeria, Energy 169 (2019) 613–624.

J. D. Fonseca, J.-M. Commenge, M. Camargo, L. Falk, I. D. Gil, Multi-criteria optimization for the design and operation of distributed energy systems considering sustainability dimensions, Energy 214 (2021) 118989.

A. Ayse Fidan, K. Muhsin, Design and performance evaluation based on economics and environmental impact of a pv-wind-diesel and battery standalone power system for various climates in turkey, Renewable Energy 157 (2020) 424–443.

R. D. Bingham, M. Agelin-Chaab, M. A. Rosen, Whole building optimization of a residential home with pv and battery storage in the bahamas, Renewable Energy 132 (2019) 1088–1103.

J. Salehi, A. Namvar, F. S. Gazijahani, Scenario-based co-optimization of neighboring multi carrier smart buildings under demand response exchange, Journal of Cleaner Production 235 (2019) 1483–1498.

Y. E. García-Vera, R. Dufo-López, J. L. Bernal-Agustín, Optimization of isolated hybrid microgrids with renewable energy based on different battery models and technologies, Energies 13 (2020) 581.

A. S. Aziz, M. F. N. Tajuddin, M. R. Adzman, A. Azmi, M. A. Ramli, Optimization and sensitivity analysis of standalone hybrid energy systems for rural electrification: A case study of iraq, Renewable energy 138 (2019) 775–792.

H. Pandžić, Optimal battery energy storage investment in buildings, Energy and Buildings 175 (2018) 189–198.

E. O'Shaughnessy, D. Cutler, K. Ardani, R. Margolis, Solar plus: Optimization of distributed solar pv through battery storage and dispatchable load in residential buildings, Applied Energy 213 (2018) 11–21.

C.-L. Nguyen, H.-H. Lee, T.-W. Chun, Cost-optimized battery capacity and short-term power dispatch control for wind farm, IEEE Transactions on Industry Applications 51 (2014) 595–606.

V. S. Borra, K. Debnath, Comparison between the dynamic programming and particle swarm optimization for solving unit commitment problems, in: 2019 IEEE Jordan International Joint Conference on Electrical Engineering and Information Technology (JEEIT), IEEE, 2019, pp. 395–400.

P. Arévalo, D. Benavides, J. Lata-García, F. Jurado, Energy control and size optimization of a hybrid system (photovoltaic-hidrokinetic) using various storage technologies, Sustainable Cities and Society 52 (2020) 101773.

B. A. Bhayo, H. H. Al-Kayiem, S. I. Gilani, F. B. Ismail, Power management optimization of hybrid solar photovoltaic-battery integrated with pumped-hydro-storage system for standalone electricity generation, Energy Conversion and Management 215 (2020) 112942.

N. Haidar, M. Attia, S.-M. Senouci, E.-H. Aglzim, A. Kribeche, Z. B. Asus, New consumer-dependent energy management system to reduce cost and carbon impact in smart buildings, Sustainable Cities and Society 39 (2018) 740–750.

K. Mahmud, M. J. Hossain, G. E. Town, Peak-load reduction by coordinated response of photovoltaics, battery storage, and electric vehicles, IEEE Access 6 (2018) 29353–29365.

J. Liu, X. Chen, H. Yang, Y. Li, Energy storage and management system design optimization for a photovoltaic integrated low-energy building, Energy 190 (2020) 116424.

P. Nagapurkar, J. D. Smith, Techno-economic optimization and environmental life cycle assessment (lca) of microgrids located in the us using genetic algorithm, Energy Conversion and Management 181 (2019) 272–291.

Z. T. Olivieri, K. McConky, Optimization of residential battery energy storage system scheduling for cost and emissions reductions, Energy and Buildings 210 (2020) 109787.

W. L. Schram, T. AlSkaif, I. Lampropoulos, S. Henein, W. G. Van Sark, On the trade-off between environmental and economic objectives in community energy storage operational optimization, IEEE Transactions on Sustainable Energy 11 (2020) 2653–2661.

V. Stepaniuk, J. Pillai, B. Bak-Jensen, Battery energy storage management for smart residential buildings, in: 2018 53rd International Universities Power Engineering Conference (UPEC), IEEE, 2018, pp. 1–6.

T. Terlouw, T. AlSkaif, C. Bauer, W. Van Sark, Multi-objective optimization of energy arbitrage in community energy storage systems using different battery technologies, Applied energy 239 (2019a) 356–372.

T. Terlouw, T. AlSkaif, C. Bauer, W. van Sark, Optimal energy management in all-electric residential energy systems with heat and electricity storage, Applied Energy 254 (2019b) 113580.

H. Moradi, A. Abtahi, M. Esfahanian, Optimal operation of a multi-source microgrid to achieve cost and emission targets, in: 2016 IEEE Power and Energy Conference at Illinois (PECI), IEEE, 2016, pp. 1–6.

A. Nottrott, J. Kleissl, B. Washom, Energy dispatch schedule optimization and cost benefit analysis for grid-connected, photovoltaic-battery storage systems, Renewable Energy 55 (2013) 230–240.

M. Yadav, M. Jamil, M. Rizwan, Accomplishing approximately zero energy buildings with battery storage using flann optimization, in: 2018 International Conference on Advances in Computing, Communication Control and Networking (ICACCCN), IEEE, 2018, pp. 656–661.

U. Mulleriyawage, W. Shen, Optimally sizing of battery energy storage capacity by operational optimization of residential pv-battery systems: An australian household case study, Renewable Energy 160 (2020) 852–864.

G. Litjens, E. Worrell, W. van Sark, Assessment of forecasting methods on performance of photovoltaic-battery systems, Applied Energy 221 (2018) 358–373.

T. Adefarati, S. Potgieter, R. Bansal, R. Naidoo, R. Rizzo, P. Sanjeevikumar, Optimization of pv-wind-battery storage microgrid system utilizing a genetic algorithm, in: 2019 International Conference on Clean Electrical Power (ICCEP), IEEE, 2019, pp. 633–638.

A. S. Aziz, M. F. N. Tajuddin, M. R. Adzman, M. A. Ramli, S. Mekhilef, Energy management and optimization of a pv/diesel/battery hybrid energy system using a combined dispatch strategy, Sustainability 11 (2019) 683.

P. García-Triviño, L. M. Fernández-Ramírez, A. J. Gil-Mena, F. Llorens-Iborra, C. A. García-Vázquez, F. Jurado, Optimized operation combining costs, efficiency and lifetime of a hybrid renewable energy system with energy storage by battery and hydrogen in grid-connected applications, International Journal of Hydrogen Energy 41 (2016) 23132–23144.

M. Marzband, E. Yousefnejad, A. Sumper, J. L. Domínguez-García, Real time experimental implementation of optimum energy management system in standalone microgrid by using multi-layer ant colony optimization, International Journal of Electrical Power & Energy Systems 75 (2016) 265–274.

M. Marzband, H. Alavi, S. S. Ghazimirsaeid, H. Uppal, T. Fernando, Optimal energy management system based on stochastic approach for a home microgrid with integrated responsive load demand and energy storage, Sustainable cities and society 28 (2017) 256–264.

A. González-Briones, J. Prieto, F. De La Prieta, E. Herrera-Viedma, J. M. Corchado, Energy optimization using a case-based reasoning strategy, Sensors 18 (2018) 865.

L. Luo, S. S. Abdulkareem, A. Rezvani, M. R. Miveh, S. Samad, N. Aljojo, M. Pazhoohesh, Optimal scheduling of a renewable based microgrid considering photovoltaic system and battery energy storage under uncertainty, Journal of Energy Storage 28 (2020) 101306.

J. A. Auñón-Hidalgo, M. Sidrach-de Cardona, F. Auñón-Rodríguez, Performance and co2 emissions assessment of a novel combined solar photovoltaic and thermal, with a stirling engine micro-chp system for domestic environments, Energy Conversion and Management 230 (2021) 113793.

G. S. Georgiou, P. Christodoulides, S. A. Kalogirou, Optimizing the energy storage schedule of a battery in a pv grid-connected nzeb using linear programming, Energy 208 (2020a) 118177.

G. S. Georgiou, P. Nikolaidis, S. A. Kalogirou, P. Christodoulides, A hybrid optimization approach for autonomy enhancement of nearly-zero-energy buildings based on battery performance and artificial neural networks, Energies 13 (2020b).

H. Zhang, A. Davigny, F. Colas, Y. Poste, B. Robyns, Fuzzy logic based energy management strategy for commercial buildings integrating photovoltaic and storage systems, Energy and Buildings 54 (2012) 196–206.

V. V. V. S. N. Murty, A. Kumar, Optimal energy management and techno-economic analysis in microgrid with hybrid renewable energy sources, Journal of Modern Power Systems and Clean Energy 8 (2020) 929–940.

C. Feng, Y. Wang, Q. Chen, Y. Ding, G. Strbac, C. Kang, Smart grid encounters edge computing: Opportunities and applications, Advances in Applied Energy 1 (2021) 100006.

S. Siami-Namini, N. Tavakoli, A. Siami Namin, A comparison of arima and lstm in forecasting time series, in: 17th IEEE International Conference on Machine Learning and Applications (ICMLA), 2018, pp. 1394–1401. doi:10.1109/ICMLA.2018.00227.

A. Monacchi, D. Egarter, W. Elmenreich, S. D'Alessandro, A. M. Tonello, Greend: An energy consumption dataset of households in italy and austria, in: IEEE International Conference on Smart Grid Communications, 2014, pp. 511–516.

UKDALE, The uk-dale dataset, domestic appliance-level electricity demand and whole-house demand from five uk homes, 2015. URL: https://doi.org/10.1038/sdata.2015.7.

IHEPCDS, Individual household electric power consumption data set, 2010. URL: https://archive.ics.uci.edu/ml/datasets/.

NREL, Pvwatts calculator, 2020. URL: https://pvwatts.nrel.gov/pvwatts.php.

Pvgis photovoltaic geographical information system, 2020. URL: https://ec.europa.eu/jrc/en/pvgis.

Carbon intensity api, 2020. URL: https://carbonintensity.org.uk.

2022. URL: https://www.rte-france.com/eco2mix.

Statista, Le prix de l'électricité en europe, 2021. URL: https://fr.statista.com/infographie/11825/.

A. A. Shukhobodskiy, A. Zaitcev, T. Pogarskaia, G. Colantuono, Red wolf hybrid storage system: Comparison of co2 and price targets, Journal of Cleaner Production 321 (2021) 128926.

D. N. Karamov, K. V. Suslov, Structural optimization of autonomous photovoltaic systems with storage battery replacements, Energy Reports 7 (2021) 349–358.

P. Nain, A. Kumar, A state-of-art review on end-of-life solar photovoltaics, Journal of Cleaner Production (2022) 130978.

V. Sebestyén, Renewable and sustainable energy reviews: Environmental impact networks of renewable energy power plants, Renewable and Sustainable Energy Reviews 151 (2021) 111626.